

# Quantum Coherence of Top Quark Pairs Produced at LHC

Saeed Haddadi<sup>1,\*</sup>, Majid Azizi<sup>1</sup> and Artur Czerwinski<sup>2,3</sup>

<sup>1</sup>*School of Particles and Accelerators, Institute for Research in Fundamental Sciences (IPM), P.O. Box 19395-5531, Tehran, Iran*

<sup>2</sup>*Institute of Physics, Faculty of Physics, Astronomy and Informatics, Nicolaus Copernicus University in Torun, ul. Grudziadzka 5, 87-100 Torun, Poland*

<sup>3</sup>*STARTOVA UMK Sp. z o.o., ul. Gagarina 7, 87-100 Torun, Poland*

(Dated: February 25, 2026)

We study quantum coherence in top–antitop production at the LHC by comparing Standard Model predictions with CMS data across different kinematic regimes. Theory and experiment are statistically consistent in the near-threshold and boosted central regions, confirming that the spin-density framework captures the dominant helicity-interference structure. The intermediate-mass window shows a noticeable deviation, indicating enhanced sensitivity to radiative QCD effects. This work reinterprets measured spin-correlation data within a quantum-coherence framework, thereby introducing coherence as a complementary and experimentally grounded probe of the Standard Model spin structure and a potentially sensitive diagnostic of new-physics effects in the top-quark sector.

*Introduction*— Quantum coherence is a foundational feature of quantum theory, representing the ability of quantum systems to exhibit superpositions between different basis states [1]. In recent years, the study of entanglement [2] has extended into the domain of high-energy physics, including analyses of spin-correlated states in top-quark pairs produced at the Large Hadron Collider (LHC) [3–9]. Unlike entanglement, which describes nonclassical correlations between subsystems, quantum coherence is a more general resource, present even in single-particle states and essential for the manifestation of all other quantum correlations [10, 11]. This broader scope places coherence at the base of the hierarchy of quantum resources, with entanglement and nonlocality emerging only under more restrictive structural conditions [12, 13]. A general hierarchical classification of quantum resources can be expressed as follows: Bell nonlocality  $\subseteq$  quantum steering  $\subseteq$  entanglement  $\subseteq$  quantum discord  $\subseteq$  quantum coherence.

While entanglement and other quantum correlations have been successfully identified in the spin configurations of top-quark pairs created in high-energy collisions [14–18], we are motivated to investigate quantum coherence as a more encompassing indicator of quantum behavior in such systems. Quantum coherence, being basis-dependent and intrinsically connected to quantum interference phenomena, provides a richer framework for analyzing the quantum properties of top pairs, especially in scenarios where entanglement may be absent or obscured by noise and decoherence mechanisms inherent to collider environments.

Bell nonlocality, a stricter form of quantum correlation which reveals the incompatibility of quantum predictions with local hidden variable models, has also been investigated in particle systems such as  $B$  mesons [19], charmonia [20], and so on [21–29]. However, the presence of Bell nonlocality implies entanglement but not vice versa, and similarly, entanglement implies coherence but not the converse. Thus, quantum coherence encompasses a broader class of quantum states, including those which are entangled or nonlocal as well as those which are not. In the context of top-quark pairs, coherence may therefore persist across a wider region of phase space, offering deeper insights into the quantum dynamics of the system.

In this Letter, we examine the quantum coherence encoded in the spin degrees of freedom of top-quark pairs produced at the LHC. We analyze how coherence varies with the kinematic parameters of the production process and demonstrate that coherent spin states can exist even in regions where entanglement fails standard detection criteria. Unlike entanglement, which is strongly reduced by mixedness or partial tracing, coherence can remain robust, making it a valuable probe of quantum features in the noisy environment of collider experiments. Our analysis builds upon measured angular distributions in top-quark decay channels to reconstruct the spin density matrix and quantify coherence. Motivated by the recent CMS measurements of the full set of spin-correlation coefficients, we perform a direct comparison between Standard Model (SM) predictions and experimental data, thereby elevating quantum coherence from a purely theoretical construct to an experimentally testable observable. This data-driven framework establishes coherence as a practical probe of QCD helicity interference and a novel

---

\* haddadi@ipm.ir

tool for exploring possible deviations from the SM in the top-quark sector.

*Methods*— A pair of top and antitop quarks, each with spin half, provides a natural realization of a two-qubit system. At the LHC, such pairs are produced in high-energy proton–proton collisions. Protons are made of quarks and gluons, collectively known as partons, whose momentum distribution inside the proton is described by the parton distribution function (PDF). Top–antitop ( $t\bar{t}$ ) pairs mainly

originate from parton-level interactions governed by QCD, such as gluon–gluon fusion ( $gg \rightarrow t\bar{t}$ ) and quark–antiquark annihilation ( $q\bar{q} \rightarrow t\bar{t}$ ). In the center-of-mass frame, the production kinematics are characterized by the invariant mass of the top-quark pair  $M_{t\bar{t}}$  and the related scattering angle  $\Theta$ .

The density matrix describing the spin state of a system formed by two spin-1/2 particles, a bipartite qubit system, can be generically written in the Hilbert–Schmidt basis as

$$\rho = \frac{1}{4} \left( \mathbb{I}_2 \otimes \mathbb{I}_2 + \sum_{i=1}^3 B_i^+ \sigma_i \otimes \mathbb{I}_2 + \sum_{j=1}^3 B_j^- \mathbb{I}_2 \otimes \sigma_j + \sum_{i,j=1}^3 C_{ij} \sigma_i \otimes \sigma_j \right), \quad (1)$$

where  $\sigma_i$  denote the Pauli matrices and  $\mathbb{I}_2$  is a  $2 \times 2$  identity matrix.  $B_i^+$  and  $B_i^-$  are the polarization state of the single particles, and  $C_{ij}$  form the spin-spin correlation matrix  $C$ . The components  $C_{ij}$  encapsulate the essential quantum correlations in the joint spin state, and are experimentally reconstructed through angular correlations in the decay products of the top quark. In the helicity basis, the production spin density matrix is fully described by five parameters, as the net polarizations vanish at leading order (LO). The analytical forms of these parameters for the  $gg$  and  $q\bar{q}$  channels are provided in Ref. [3], expressed in terms of the top-quark velocity  $\beta = \sqrt{1 - 4m_t^2/M_{t\bar{t}}^2}$  and the production angle. Note that the production threshold ( $\beta = 0$ ) occurs at  $M_{t\bar{t}} = 2m_t \approx 346$  GeV where  $m_t$  is the top quark’s mass.

Based on a combination of experimental data and theoretical QCD predictions, about 90% of  $t\bar{t}$  pairs produced at the LHC ( $\sqrt{s} = 13$  TeV) originate from  $gg \rightarrow t\bar{t}$ , with the remainder arising from  $q\bar{q} \rightarrow t\bar{t}$  [30].

To quantify the quantum coherence present in the spin state of top-quark pairs, we adopt the  $l_1$ -norm of coherence, a widely used measure within the resource theory of coherence [1]. For a given density matrix  $\rho$ , the  $l_1$ -norm of coherence is defined as

$$\mathcal{C}_{l_1}(\rho) = \sum_{i \neq j} |\rho_{ij}|, \quad (2)$$

where the summation runs over all off-diagonal elements of  $\rho$  in a fixed reference basis. This quantity captures the total amount of coherence by summing the absolute values of all off-diagonal terms.

*Results*— Figure 1 provides the dependence of the  $l_1$ -norm of quantum coherence on the scattering angle (through  $\cos \Theta$ ) and on the invariant mass  $M_{t\bar{t}}$  of

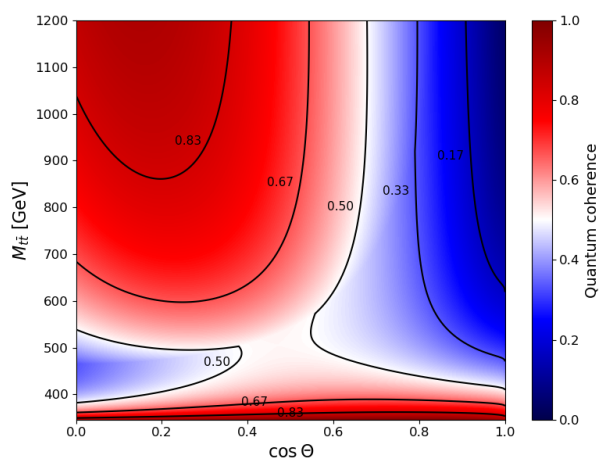


FIG. 1. The behavior of the  $l_1$ -norm of coherence over the considered kinematic space for top–antitop ( $t\bar{t}$ ) production at the LHC.

the top–antitop quark pair produced at the LHC. In the low-mass regime ( $346 < M_{t\bar{t}} < 400$  GeV), the  $t\bar{t}$  pair is produced close to threshold, where the available phase space is limited and spin correlations between the quark and antiquark remain strong. The  $l_1$ -norm of coherence is relatively high, with small angular dispersion. This high coherence near threshold can be attributed to the near-resonant production channel, where the system remains dynamically correlated and less affected by random phase fluctuations from the partonic environment. As the invariant mass increases (intermediate regime,  $400 < M_{t\bar{t}} < 600$  GeV), the phase space for gluon radiation and higher-order QCD effects becomes larger, leading to a partial loss of quantum coherence. The average  $l_1$ -norm of coherence decreases moderately, and

TABLE I. The  $l_1$ -norm of quantum coherence (mean values) as obtained through the theoretical calculations (Fig. 1) and experimental (CMS) data pertaining to the three bins.

Bins	$M_{t\bar{t}}$ (GeV)	$\cos \Theta$	Theor.	Exp.
Threshold	346 – 400	0 – 1	$0.71 \pm 0.28$	$0.80 \pm 0.19$
Intermediate	400 – 600	0 – 1	$0.47 \pm 0.24$	$0.90 \pm 0.07$
Boosted central	> 800	< 0.4	$0.83 \pm 0.08$	$1.07 \pm 0.23$

the dependence on  $\cos \Theta$  becomes more pronounced. This suggests that forward- and backward-scattering events begin to differ significantly in their coherent character. Although coherence decreases, it remains nonzero across all scattering angles, indicating the persistence of intrinsic quantum superpositions within the production channel. Next, events with central scattering angles ( $\cos \Theta < 0.4$ ) and large invariant masses ( $M_{t\bar{t}} > 800$  GeV) show consistently large values of the  $l_1$ -norm of quantum coherence. The coherence in this boosted central bin has a small dispersion, indicating a robust, repeatable effect in that kinematic window. One might expect that raising  $M_{t\bar{t}}$  increases radiation and therefore decoherence. Instead, the calculations show that for central angles, increasing the invariant mass does not destroy coherence, but rather enhances or preserves it. The small spread (low variance) of coherence in this region shows that the constructive interference is not a rare fluctuation but a stable feature of the underlying production dynamics at high  $M_{t\bar{t}}$ .

The complete set of coefficients  $B_i^\pm$  and  $C_{ij}$  appearing in Eq. (1), which fully characterize the spin density matrix of the top–antitop ensemble, has recently been reported by the CMS Collaboration [9]. This enables a direct comparison between our analytic predictions from the previous section and experimental data [31]. To perform this test, we recast the CMS measurements in terms of the corresponding quantum coherence values obtained on the helicity basis, as summarized in Table I. For a precise comparison, we propagate the quoted uncertainties of the  $B_i^\pm$  and  $C_{ij}$  coefficients [32] corresponding to the bins included in our analysis. This table shows an overall good consistency between the theoretical predictions (Fig. 1) and the CMS experimental measurements of the  $l_1$ -norm of quantum coherence, with the level of agreement depending on the kinematic regime.

In the threshold region ( $346 < M_{t\bar{t}} < 400$  GeV), the theoretical mean value  $0.71 \pm 0.28$  is fully consistent with the experimental result  $0.80 \pm 0.19$  within uncertainties. The central values are close, and the combined error bars largely overlap. This agreement supports the interpretation that near-threshold production is dominated by strong spin correlations and

coherent helicity interference, with limited phase space suppressing decohering radiation. The data confirm that the theoretical spin-density description captures the essential dynamics in this regime.

In the intermediate-mass region ( $400 < M_{t\bar{t}} < 600$  GeV), the theoretical prediction  $0.47 \pm 0.24$  is significantly lower than the CMS value  $0.90 \pm 0.07$ . Although coherence remains nonzero in both cases, the experimental result indicates a substantially larger magnitude. This suggests that the intermediate window is particularly sensitive to radiative QCD effects, angular averaging, and possibly higher-order contributions that are not fully captured at the level of our present LO theoretical modeling. Importantly, even in this region—where entanglement has been reported to be nearly vanishing using the same CMS data (see recent paper [29])—the measured coherence remains sizable, confirming that quantum coherence survives beyond the entanglement-detection threshold and provides additional structural information about the spin-density matrix.

In the boosted central region ( $M_{t\bar{t}} > 800$  GeV,  $\cos \Theta < 0.4$ ), theory predicts a large coherence  $0.83 \pm 0.08$ , while the experimental value  $1.07 \pm 0.23$  is even larger but compatible within uncertainties. Both results consistently indicate enhanced coherence in this kinematic domain. This confirms that increasing invariant mass does not necessarily induce monotonic decoherence; rather, for central scattering angles, constructive helicity interference remains effective and may even be amplified. The relatively small theoretical dispersion further supports the interpretation that the enhancement is a stable dynamical feature rather than a statistical fluctuation.

The comparison reveals that the theoretical description reproduces the experimental data with very high accuracy in the threshold and boosted-central regimes, while the intermediate-mass region shows a moderate deviation, highlighting it as the most sensitive domain for improving theoretical precision.

The analysis of quantum coherence in top–antitop production offers a direct and highly nontrivial probe of the spin dynamics predicted by the SM. In proton–proton collisions at the LHC,  $t\bar{t}$  pairs are produced predominantly via gluon–gluon fusion, a process dictated by the  $SU(3)_c$  gauge symmetry of QCD [33]. The Lorentz and gauge structure of the top–gluon vertex fully determines the helicity amplitudes, and consequently fixes the form of the spin density matrix describing the produced  $t\bar{t}$  system. The off-diagonal components of this density matrix, quantified through the  $l_1$ -norm of coherence, originate from interference among distinct helicity configurations in the QCD production amplitude. Hence, both the magnitude and the kinematic behavior of

quantum coherence provide a direct window into the vector character of the gluon coupling, angular momentum conservation, and the unitarity of the underlying quantum field-theoretic framework.

The observation that coherence remains substantial in both the near-threshold and boosted central regimes is fully consistent with the SM expectation that spin correlations arise from coherent quantum superpositions of partonic helicity states rather than from incoherent classical mixtures. Any significant deviation in the dependence of coherence on  $M_{t\bar{t}}$  or  $\cos\Theta$  would therefore point to possible new-physics effects, such as anomalous chromomagnetic or chromoelectric dipole couplings, contributions from higher-dimensional operators within an effective field theory description, or unexpected decoherence mechanisms in the top-quark sector. In this context, quantum coherence serves as a complementary observable to traditional spin-correlation analyses. While entanglement measurements probe the nonseparability of the state, coherence quantifies the full interference structure encoded in the production amplitudes. The good agreement between theoretical predictions and CMS data reported in Table I thus provides further independent support for the SM description of top-quark pair production at TeV-scale energies. Moreover, the persistence of large coherence in boosted central kinematics—despite the enlarged phase space for QCD radiation—reinforces the stability of the SM spin-interference pattern and constrains scenarios in which new physics would induce partial decoherence in the top sector.

*Summary*— In this Letter, we have demonstrated that quantum coherence in  $t\bar{t}$  production exhibits a non-monotonic dependence on invariant mass and scattering angle, dictated by the interference struc-

ture of QCD helicity amplitudes. The strong agreement between theoretical predictions and CMS data in the threshold and boosted central regimes confirms the robustness of the SM spin-density description, while the intermediate-mass region reveals enhanced sensitivity to radiative dynamics. Since coherence directly probes the off-diagonal elements of the spin density matrix, it accesses the full interference structure of the production amplitudes and therefore contains information beyond conventional spin-correlation observables. Importantly, our work goes beyond previous studies that focused primarily on formal calculations of quantum information measures without confronting data or extracting phenomenological implications. Here, we have performed a direct theory–experiment comparison and, based on the observed kinematic patterns, proposed concrete strategies for using quantum coherence and quantum correlations of top quarks as discovery tools. In particular, we identify specific invariant-mass and angular regions where coherence is maximally sensitive to deviations from the SM, thereby providing experimentally testable benchmarks for anomalous couplings, higher-dimensional operators, or decoherence effects in the top sector. By embedding quantum information concepts into collider phenomenology with explicit experimental validation and predictive guidance, our results establish quantum coherence as a precision and practically deployable probe for uncovering new physics at TeV energies.

*Acknowledgments*— We would like to express our sincere gratitude to Prof. Mojtaba Mohammadi Najafabadi for his insightful and constructive comments. S.H. and M.A. also thank the School of Particles and Accelerators at the Institute for Research in Fundamental Sciences (IPM) for their financial support of this project.

- 
- [1] T. Baumgratz, M. Cramer, and M. B. Plenio, Quantifying coherence, *Phys. Rev. Lett.* **113**, 140401 (2014).
  - [2] R. Horodecki, P. Horodecki, M. Horodecki, and K. Horodecki, Quantum entanglement, *Rev. Mod. Phys.* **81**, 865 (2009).
  - [3] Y. Afk and J. R. M. de Nova, Entanglement and quantum tomography with top quarks at the LHC, *Eur. Phys. J. Plus* **136**, 907 (2021).
  - [4] M. Fabbrichesi, R. Floreanini, and E. Gabrielli, Constraining new physics in entangled two-qubit systems: top-quark, tau-lepton and photon pairs, *Eur. Phys. J. C* **83**, 162 (2023).
  - [5] I. Georgescu, Entanglement between a pair of top quarks, *Nat. Rev. Phys.* **6**, 85 (2024).
  - [6] A. J. Barr, M. Fabbrichesi, R. Floreanini, E. Gabrielli, and L. Marzola, Quantum entanglement and Bell inequality violation at colliders, *Prog. Part. Nucl. Phys.* **139**, 104134 (2024).
  - [7] The ATLAS Collaboration, Observation of quantum entanglement with top quarks at the ATLAS detector, *Nature* **633**, 542–547 (2024).
  - [8] The CMS Collaboration, Observation of quantum entanglement in top quark pair production in proton–proton collisions at  $\sqrt{s} = 13$  TeV, *Rep. Prog. Phys.* **87**, 117801 (2024).
  - [9] The CMS Collaboration, Measurements of polarization and spin correlation and observation of entanglement in top quark pairs using lepton+ jets events from proton-proton collisions at  $\sqrt{s} = 13$  TeV, *Phys. Rev. D* **110**, 112016 (2024).
  - [10] A. Streltsov, G. Adesso, and M. B. Plenio, Col-

- loquium: Quantum coherence as a resource, *Rev. Mod. Phys.* **89**, 041003 (2017).
- [11] M.-L. Hu, X. Hu, J. Wang, Y. Peng, Y.-R. Zhang, and H. Fan, Quantum coherence and geometric quantum discord, *Phys. Rep.* **762-764**, 1 (2018), quantum coherence and geometric quantum discord.
- [12] H. M. Wiseman, S. J. Jones, and A. C. Doherty, Steering, entanglement, nonlocality, and the Einstein-Podolsky-Rosen paradox, *Phys. Rev. Lett.* **98**, 140402 (2007).
- [13] G. Adesso, T. R. Bromley, and M. Cianciaruso, Measures and applications of quantum correlations, *J. Phys. A: Math. Theor.* **49**, 473001 (2016).
- [14] Y. Afik and J. R. M. de Nova, Quantum discord and steering in top quarks at the LHC, *Phys. Rev. Lett.* **130**, 221801 (2023).
- [15] J. Datta, A. Deshpande, D. E. Kharzeev, C. J. Naïm, and Z. Tu, Entanglement as a probe of hadronization, *Phys. Rev. Lett.* **134**, 111902 (2025).
- [16] K. Cheng, T. Han, and M. Low, Optimizing entanglement and Bell inequality violation in top antitop events, *Phys. Rev. D* **111**, 033004 (2025).
- [17] B.-L. Ye, L.-Y. Xue, Z.-Q. Zhu, D.-D. Shi, and S.-M. Fei, Entropic uncertainty relations and quantum Fisher information of top quarks in a large hadron collider, *Phys. Rev. D* **110**, 055025 (2024).
- [18] S. Rai and J. Kumar, Nonlocal advantage of quantum coherence in top quarks, *Phys. Rev. D* **112**, 114043 (2025).
- [19] M. Fabbrichesi, R. Floreanini, E. Gabrielli, and L. Marzola, Bell inequality is violated in  $B^0 \rightarrow j/\psi K^*(892)^0$  decays, *Phys. Rev. D* **109**, L031104 (2024).
- [20] M. Fabbrichesi, R. Floreanini, E. Gabrielli, and L. Marzola, Bell inequality is violated in charmonium decays, *Phys. Rev. D* **110**, 053008 (2024).
- [21] M. Fabbrichesi, R. Floreanini, and G. Panizzo, Testing Bell inequalities at the LHC with top-quark pairs, *Phys. Rev. Lett.* **127**, 161801 (2021).
- [22] Y. Afik and J. R. M. de Nova, Quantum information with top quarks in QCD, *Quantum* **6**, 820 (2022).
- [23] C. Severi, C. D. E. Boschi, F. Maltoni, and M. Sioli, Quantum tops at the LHC: from entanglement to Bell inequalities, *Eur. Phys. J. C* **82**, 285 (2022).
- [24] J. A. Aguilar-Saavedra and J. A. Casas, Improved tests of entanglement and Bell inequalities with LHC tops, *Eur. Phys. J. C* **82**, 666 (2022).
- [25] Z. Dong, D. Gonçalves, K. Kong, and A. Navarro, Entanglement and Bell inequalities with boosted  $t\bar{t}$ , *Phys. Rev. D* **109**, 115023 (2024).
- [26] T. Han, M. Low, and T. A. Wu, Quantum entanglement and Bell inequality violation in semi-leptonic top decays, *J. High Energ. Phys.* **2024**, 192.
- [27] S. Wu, C. Qian, Q. Wang, and X.-R. Zhou, Bell nonlocality and entanglement in  $e^+e^- \rightarrow \eta\bar{Y}$  at BESIII, *Phys. Rev. D* **110**, 054012 (2024).
- [28] R. Demina and G. Landi, Locality in collider tests of quantum mechanics with top quark pairs, *Phys. Rev. D* **111**, 012013 (2025).
- [29] M. Fabbrichesi, R. Floreanini, and L. Marzola, Local vs. nonlocal entanglement in top-quark pairs at the LHC, *J. High Energ. Phys.* **2025**, 5.
- [30] S. Navas and et al. (Particle Data Group Collaboration), Review of particle physics, *Phys. Rev. D* **110**, 030001 (2024).
- [31] We use the observables  $C_{nr}^\pm = C_{nr} \pm C_{rn}$ ,  $C_{rk}^\pm = C_{rk} \pm C_{kr}$ , and  $C_{nk}^\pm = C_{nk} \pm C_{kn}$ , where the associated covariances are fully taken into account in the calculation [9].
- [32] HEPdata, <https://hepdata.net/record/ins2829523>.
- [33]  $SU(3)_c$  gauge symmetry is the non-Abelian color symmetry underlying QCD, whose vector top-gluon interaction uniquely fixes the helicity amplitudes and thus determines the spin-interference structure of top-antitop production.